Experimental investigation on the variation of thermal conductivity of soils with effective stress, porosity, and water saturation

So-Jung Lee [1a], Kyoung-Yul Kim [2b], Jung-Chan Choi [3c] and Tae-Hyuk Kwon [*4]

[1] *Korea Institute of Civil Engineering and Building Technology (KICT), Daejeon, Korea*
[2] *Principle Researcher, Structural and Seismic Technology Group, Power Transmission Laboratory,*
Korea Electric Power Research Institute (KEPRI), Daejeon, Korea
[3] *Norwegian Geotechnical Institute (NGI), Oslo, Norway*
[4] *Department of Civil and Environmental Engineering, Korea Advanced Institute of*
Science and Technology (KAIST), Daejeon, Korea

Abstract. The thermal conductivity of soils is an important property in energy-related geotechnical structures, such as underground heat pumps and underground electric power cable tunnels. This study explores the effects of geotechnical engineering properties on the thermal conductivity of soils. The thermal conductivities of quartz sands and Korean weathered silty sands were documented via a series of laboratory experiments, and its variations with effective stress, porosity, and water saturation were examined. While thermal conductivity was found to increase with an increase in the effective stress and water saturation and with a decrease in porosity, replacing air by water in pores the most predominantly enhanced the thermal conductivity by almost one order of magnitude. In addition, we have suggested an improved model for thermal conductivity prediction, based on water saturation, dry thermal conductivity, saturated thermal conductivity, and a fitting parameter that represents the curvature of the thermal conductivity-water saturation relation.

Keywords: thermal conductivity; quartz sand; silty sand; weathered soil; effective stress; water saturation; correlation

1. Introduction

The thermal conductivity of soils is an important property that quantifies the ability of soils to conduct heat, as thermal conduction is the predominant heat transfer mechanism among conduction, convection, and radiation (Carslaw and Jaeger 1959, Murashov and White 2000). The estimation of the thermal conductivity of soils has gathered significant interest because the demand for energy-related geo-structures, such as underground heat pumps and underground

∗Corresponding author, Assistant Professor, E-mail: t.kwon@kaist.ac.kr
[a] Graduate Student, E-mail: sojunglee513@kaist.ac.kr
[b] Principle Researcher, E-mail: patric@kepco.co.kr
[c] Senior Researcher, E-mail: jungchan.choi@ngi.no

electric power cable tunnels, rises as some of the promising renewable energy resources or sustainable unban designs (Kumai *et al.* 1994, Brandl 2006, Johnston *et al.* 2011, Go *et al.* 2014). There have been extensive efforts to understand the inter-relations between thermal conductivity and various engineering parameters, such as mineral types, dry unit weight, porosity, and water content (e.g., Batchelor and O'Brien 1977, Sridhar and Yovanovich 1996, Gangadhara Rao and Singh 1999, Manohar *et al.* 2000, Singh and Devid 2000, Vargas and McCarthy 2001, Tarnawski *et al.* 2002, Kumultas *et al.* 2003, Andersland and Ladanyi 2004, Esch 2004, Gori and Corasaniti 2004, Lu *et al.* 2007, Yun and Santamarina 2008, Nasirian *et al.* 2015). Accordingly, it has proven that the thermal conductivity of soils is affected not only by the volumetric fractions and the bulk conductivity of each phase but also by the inherent contact conditions, such as contact area, coordination number, and presence of water menisci (Sridhar and Yovanovich 1996, Tarnawski *et al.* 2002, Kumultas *et al.* 2003, Yun and Santamarina 2008, Nasirian *et al.* 2015). While effective thermal conductivity models must consider the inherent contact conditions, their roles in soil thermal conductivity remain poorly identified.

Inherent contact conditions in soils are heavily affected by the effective stress, packing density (or porosity), and water content (or degree of saturation): the effective stress governs the grain-to-grain contact area, the porosity represents the coordination number, and the degree of saturation (or water saturation) can be related with the shape of water meniscus at the grain-to-grain contacts. Therefore, this study explored the effects of effective stress, porosity, and water saturation on the thermal conductivity of soils. The thermal conductivities of quartz sands and weathered silty sands were documented via a series of laboratory experiments. The variations in thermal conductivity with the changes in effective stress, porosity, and water saturation were examined. In addition, we suggested an improved model for thermal conductivity prediction of quartz-dominant sands and weathered silty sands with various minerals, and compared the results with the previous thermal conductivity estimation models.

2. Materials and method

2.1 Basic index and physical properties of soils used

Ottawa 20/30 sand and the weathered soil cored from Gochang, Korea were chosen for this study. Fig. 1 shows the grain size distributions of the two soil samples. The Ottawa 20/30 sand sample was round-shaped and quite uniformly graded with a mean particle size (D_{50}) of ~0.6 mm. The weathered soil sample was found to be angular-shaped, and had a wide size distribution with a mean particle size (D_{50}) of ~0.42 mm. According to the Unified Soil Classification System (USCS), the Ottawa 20/30 sample was classified as poorly graded clean sand (SP) with no fine content. The weathered soil contained a fine fraction of ~8.3%, and was classified as poorly graded sand with some silt (SP-SM). Table 1 summarizes the particle images and basic index properties of the two soil samples used in this study. More than 99% of Ottawa 20/30 sand consisted of quartz (i.e., quartz sand) and the weathered soil consisted of 39.6% quartz, 22.4% kaolinite, 18.7% microcline, 12.4% illite, 4.5% albite, 1.3% magnetite, and 1.0% biotite, which was identified via X-ray diffraction (XRD) analysis; the details are shown in Table 2. Herein, the Ottawa 20/30 sand was named as the quartz sand (QS) and the weathered soil was referred to as the weathered silty sand (WS). Among the minerals, quartz has the greatest thermal conductivity (e.g., ~7.7 $W \cdot m^{-1} \cdot K^{-1}$) and albite and biotite have the lowest (e.g., ~2.0 $W \cdot m^{-1} \cdot K^{-1}$). Therefore, if the weighted average is
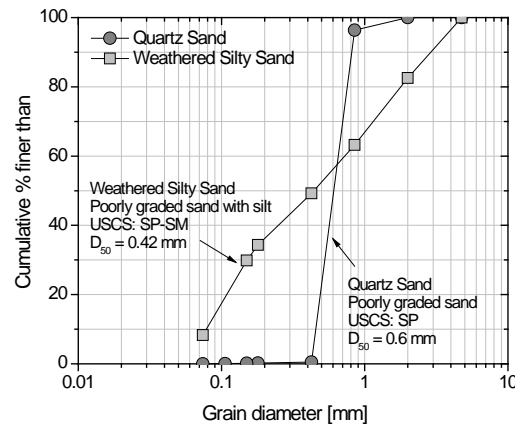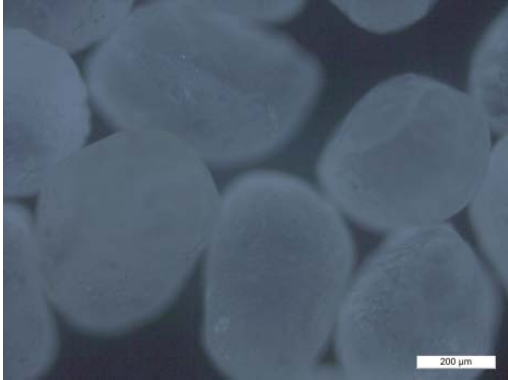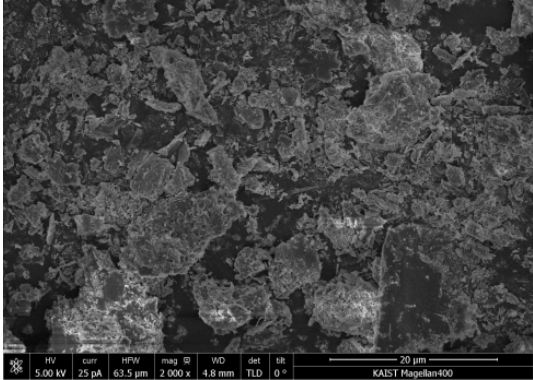
Fig. 1 Grain size distributions of the quartz sand and weathered silty sand samples

Table 1 Basic index properties and particle images of quartz sand and weathered silty sand samples

Quartz sand (Ottawa 20/30)		Weathered silty sand (from Gochang, Korea)	
D_{50} = 0.6 mm	n_{max} / n_{min} = 0.43 / 0.33 [a]	D_{50} = 0.42 mm	n_{max} / n_{min} = 0.50 / 0.31
D_{10} = 0.45 mm	G_s = 2.65	D_{10} = 0.08 mm	G_s = 2.65
C_c = 1.44	USCS: SP	C_c = 8	USCS: SP-SM
C_u = 0.92	% passing #200 sieve = 0%	C_u = 0.4	% passing #200 sieve = 8.3%

Note: [a] Yun and Santamarina (2008). D_{50} and D_{10} are the mean particle diameter and the effective particle diameter for which 50% and 10% of the particles are finer. C_c and C_u are the coefficient of curvature (i.e., $C_c = D_{30}^2 / (D_{10} \cdot D_{60})$), and the coefficient of uniformity (i.e., $C_u = D_{60}/D_{10}$). n_{max} and n_{min} are the maximum and minimum porosity obtained according to ASTM D4253-14 and ASTM D4254-14. G_s is the specific gravity of the grains

taken, the thermal conductivity of solid minerals for the weathered silty sand is calculated as ~4.7 $W·m^{-1}·K^{-1}$; this is significantly lower than that for the quartz sand (~7.7 $W·m^{-1}·K^{-1}$).

2.2 Experimental setup and procedure

Thermal needle probe method for thermal conductivity measurement:
The thermal needle probe method was chosen for measuring the thermal conductivity of soils.

Table 2 Composition, thermal conductivity and grain density of the minerals
in the weathered silty sand sample

Mineral [a]	Portion [a] [%]	Thermal conductivity [b] [W·m⁻¹·K⁻¹]	Density [b] [g/cm³]
Quartz	39.6	7.69	2.65
Kaolinite	22.4	2.61–2.68 [c]	2.6 [c]
Microcline	18.7	2.49	2.56
Muscovite/Illite	12.4	3.48	2.85
Albite	4.5	1.96	2.63
Magnetite	1.3	5.10	5.15
Biotite	1.1	2.02	2.98
Quartz	39.6	7.69	2.65

Note: [a] The mineral composition was obtained from the XRD analysis;
[b] Horai and Simmons (1969); [c] Brigaud and Vasseur (1989)

In this method, a thermal needle probe that housed a heating wire and a thermistor, as shown in Fig. 2(a), was used (Van der Held and Van Drunnen 1949, Carslaw and Jaeger 1959, von Herzen and Maxwell 1959, Woodside and Messmer 1961, Manohar *et al.* 2000, ASTM D5334-14 2014). A DC input of 2–4 V was applied to the heating wire of the probe for 180 s using a DC power supply, and the current was measured using a multimeter in order to calculate the input power to the heating wire. At the same time, the transient thermal response (i.e., temperature change) to the input power was recorded once every 50 ms with the thermistor mounted in the probe. The thermal conductivity was calculated from the acquired thermal response.
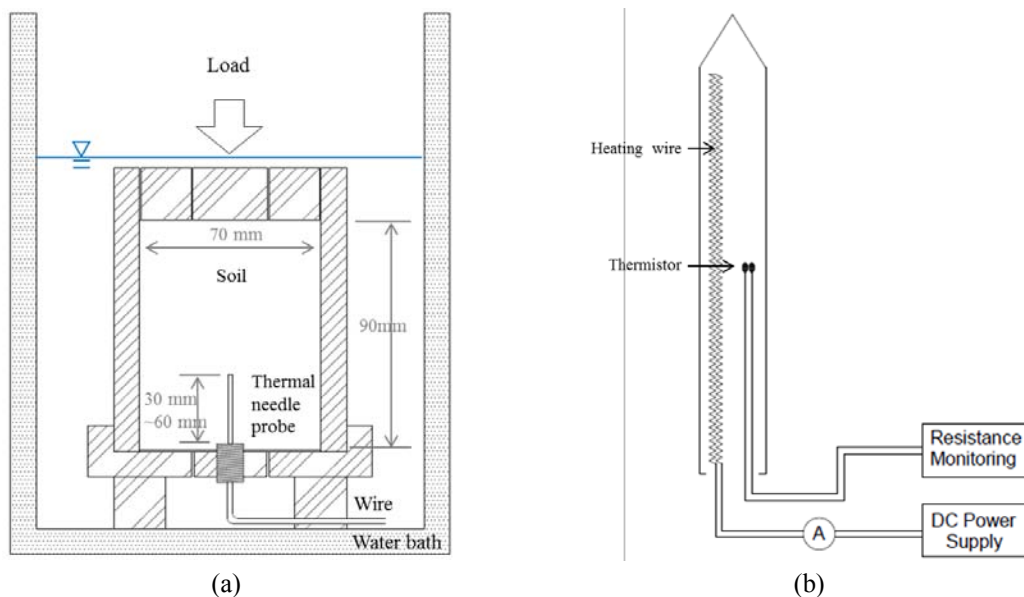

(a)   (b)

Fig. 2 (a) A schematic drawing of the test setup; and (b) the measurement system for the thermal needle probe method

Thermal needle probes: We used two types of thermal needle probes (manufactured by East 30 Sensors): one was 30 mm long, and the other was 60 mm long. The thickness of both probes was 1.58 mm, such that the length/diameter ratios were approximately 19 and 38, respectively. Calibration of both probes was conducted using materials with known thermal conductivity, such as agar (0.598 $W·m^{-1}·K^{-1}$, which is the same as for water) and glycerin (0.298 $W·m^{-1}·K^{-1}$).

Specimen preparation: An oedometric cylindrical cell, made of acrylic plastic, was used for the experiments, as shown in Fig. 2(b). The thermal needle probe was mounted at the bottom of the cell prior to packing the specimen in the cell. In the cases when the specimen is compressible enough for the probe to contact the top cap during the loading processes, the short probe was used. In all the other cases, the long probe was used. Each oven-dried soil sample was mixed thoroughly with water to achieve the target water content, and the soil-water mixture was compacted into the cell by hand-tamping. The initial heights of all the specimens were controlled to be ~90 mm, and their resulting porosities were recorded. For the preparation of completely dry specimens, no water was added, and the oven-dried soil samples were poured through a funnel, and then hand-tamped to adjust the packing density. Likewise, for fully saturated specimens, oven-dried soil samples were poured through a funnel into the cell fully filled with water, and then hand-tamped to control the packing density. Upon completion of the specimen preparation, a cap was placed on top of the specimen, and the initial thermal conductivity of the specimen was measured prior to the loading and unloading procedure. The initial conditions of the specimens are summarized in Tables 3 and 4.

Table 3 Test results complied from the quartz sand sample

QS00 (Loose)		$w_o = 0\%$		QS00 (M.Dense)		$w_o = 0\%$		QS00 (Dense)		$w_o = 0\%$	
σ'	ϕ	S	λ	σ'	Φ	S	λ	σ'	ϕ	S	λ
0.1	40.6	0	0.263	0.1	38.1	0	0.278	0.1	36.7	0	0.316
27.4	40.6	0	0.268	27.4	37.2	0	0.289	24.5	36.3	0	0.319
54.8	40.4	0	0.270	54.8	36.7	0	0.301	49.1	35.0	0	0.324
109.5	39.5	0	0.280	109.5	36.4	0	0.306	98.2	34.7	0	0.333
219.1	39.3	0	0.294	219.1	35.9	0	0.325	196.3	34.4	0	0.341
438.2	39.2	0	0.299	438.2	35.7	0	0.345	392.7	34.0	0	0.352
219.1	39.2	0	0.295	219.1	35.7	0	0.339	196.3	34.1	0	0.349
109.5	39.3	0	0.280	109.5	35.8	0	0.328	98.2	34.2	0	0.345
54.8	39.3	0	0.270	54.8	35.9	0	0.321	49.1	34.3	0	0.342
27.4	39.4	0	0.287	27.4	36.1	0	0.314	24.5	34.4	0	0.341
0.1	39.5	0	0.254	0.1	37.1	0	0.297	0.1	34.7	0	0.325
QS05		$w_o = 5.1\%$		QS10		$w_o = 9.7\%$		QS14		$w_o = 13.9\%$	
σ'	ϕ	S	λ	σ'	ϕ	S	λ	σ'	ϕ	S	λ
0.1	35.2	24.8	1.794	0.1	39	40.2	2.322	0.1	37.4	61.9	2.441
28	35	25.0	1.874	24.7	38.9	40.3	2.351	24.6	37.2	62.4	2.468
55.9	34.8	25.2	1.939	49.3	38.9	40.4	2.401	49.2	37	62.8	2.525
111.9	34.6	25.4	1.966	98.6	38.8	40.6	2.4	98.4	36.8	63.4	2.588
223.8	34.3	25.7	2.003	197.2	38.6	40.9	2.42	196.9	36.5	64.3	2.624

Table 3 Continued

QS05		w_o = 5.1%		QS10		w_o = 9.7%		QS14		w_o = 13.9%	
σ'	ϕ	S	λ	σ'	ϕ	S	λ	σ'	ϕ	S	λ
447.5	33.8	26.4	2.112	394.5	38.3	41.4	2.421	393.8	35.8	66.2	2.647
223.8	34	26.1	2.012	197.2	38.4	41.3	2.433	196.9	36.1	65.5	2.639
111.9	34.2	25.9	1.998	98.6	38.4	41.2	2.407	98.4	36.3	64.9	2.619
55.9	34.5	25.6	1.935	49.3	38.5	41.1	2.441	49.2	36.4	64.6	2.572
28	34.6	25.4	1.863	24.7	38.5	41.0	2.436	24.6	36.5	64.4	2.519
0.1	35	25.0	1.806	0.1	38.6	41.0	2.432	0.1	36.7	63.8	2.486
QS24 (Loose)		w_o = 24.1%		S21 (M.Dense)		w_o = 21.1%		QS20 (Dense)		w_o = 20.3%	
σ'	ϕ	S	λ	σ'	ϕ	S	λ	σ'	ϕ	S	λ
0.1	38.9	100	2.852	0.1	35.8	100	3.177	0.1	35.0	100	3.312
27.4	38.1	100	2.875	27.4	35.5	100	3.202	28.5	33.0	100	3.556
54.8	37.6	100	2.894	54.8	34.4	100	3.245	56.9	32.6	100	3.616
109.5	37.3	100	2.938	109.6	34.1	100	3.279	113.8	32.2	100	3.671
232.8	36.8	100	3.037	219.2	33.8	100	3.418	227.7	31.7	100	3.730
465.6	36.6	100	3.111	438.4	33.5	100	3.361	512.3	30.7	100	3.913
232.8	36.7	100	3.079	219.2	33.6	100	3.305	227.7	31.2	100	3.803
109.5	36.8	100	2.970	109.6	33.7	100	3.253	113.8	31.5	100	3.734
54.8	36.8	100	2.915	54.8	33.8	100	3.237	56.9	31.8	100	3.586
27.4	37.0	100	2.879	27.4	33.9	100	3.188	28.5	32.0	100	3.573
0.1	38.0	100	2.839	0.1	34.1	100	3.100	0.1	32.6	100	3.446

Note: w_o (%) is the initial water content of the sample prior to compaction, σ' (kPa) is the vertical effective stress, ϕ (%) is the porosity, S (%) is the water saturation (%), and λ (W·m^{-1}·K^{-1}) is the thermal conductivity

Table 4 Test results complied from the weathered silty sand sample

WS00		w_o = 0%		WS09_1		w_o = 9.0%	
σ'	ϕ	S	λ	σ'	ϕ	S	λ
0.1	43.8	0	0.313	0.1	40.2	35.5	0.726
25.3	43.6	0	0.318	28	39.3	36.8	0.737
50.6	43.0	0	0.316	55.9	38.4	38.2	0.747
101.1	42.8	0	0.328	111.9	37	40.7	0.764
202.2	42.2	0	0.343	223.8	34.6	45.1	0.847
404.4	41.6	0	0.375	447.5	29.2	57.9	1.003
202.2	41.7	0	0.38	223.8	31.4	52.0	1.001
101.1	41.7	0	0.377	111.9	32.1	50.5	0.999
50.6	41.8	0	0.374	55.9	32.6	49.2	0.999
25.3	41.8	0	0.357	28	33.1	48.2	0.984
0.1	41.9	0	0.388	0.1	34.1	46.1	0.96

Table 4 Continued

WS09_2		$w_o = 9.0\%$		WS26		$w_o = 26.0\%$	
σ'	ϕ	S	λ	σ'	ϕ	S	λ
0.1	40.2	35.5	0.877	0.1	44.3	86.8	1.375
28	40	35.8	0.917	24.6	43.2	90.7	1.423
55.9	39.1	37.1	0.928	49.2	42	95.2	1.459
111.9	37.9	39.1	0.943	98.4	40.4	100	1.525
223.8	36.1	42.2	0.984	196.9	38.7	100	1.47
447.5	34.7	44.9	1.067	393.8	35.3	100	1.539
223.8	35.4	43.6	1.089	196.9	36.3	100	1.584
111.9	36	42.4	1.088	98.4	36.9	100	1.539
55.9	36.5	41.4	1.077	49.2	37.3	100	1.552
28	37.1	40.5	1.071	24.6	37.7	100	1.56
0.1	37.8	39.3	1.063	0.1	38.6	100	1.571

Note: w_o (%) is the initial water content of the sample prior to compaction, σ' (kPa) is the vertical effective stress, ϕ (%) is the porosity, S (%) is the water saturation (%), and λ (W·m^{-1}·K^{-1}) is the thermal conductivity

Experimental procedure: A loading and unloading procedure (five loading steps) was applied to ~400 kPa to investigate the effect of effective stress on thermal conductivity. At each loading step, the thermal conductivity was measured three times, and the averaged thermal conductivity value was used for the analysis. During the loading and unloading procedure, the variations in porosity were determined from the changes in the specimen height, monitored using a dial gauge.

3. Results and analysis

3.1 Effect of effective stress σ' on thermal conductivity λ

Fig. 3 shows the variations in thermal conductivity λ with the vertical effective stress σ' during the loading and unloading steps. A general trend of increasing thermal conductivity λ with increasing effective stress σ' was observed in all the specimens of the quartz sand and weathered silty sand samples. It is because the increase in σ' increased the grain-to-grain contact area and the coordination number (or contact number), reducing the porosity (or void ratio) of the specimens (Batchelor and O'Brien 1977, Sdrdhar and Yovanovich 1996, Vargas and McCarth 2001, Yun and Santamarina 2008). For the tested σ' range up to ~400–500 kPa, the maximum variation of λ appears to be limited to ~10–25%. On the other hand, the relative increase of λ by replacing air by water was much more substantial than that by increasing effective stress, as shown in Figs. 3(c) and (d). This is consistent with Cortes *et al*. (2009) and Roshankhah and Santamarina (2014).

Moreover, the effect of pre-loading was also found, where λ on the unloading path was greater than λ on the loading process. It is presumed because such pre-loading densified the granular packing and thus increased porosity ϕ and λ for a given σ'.
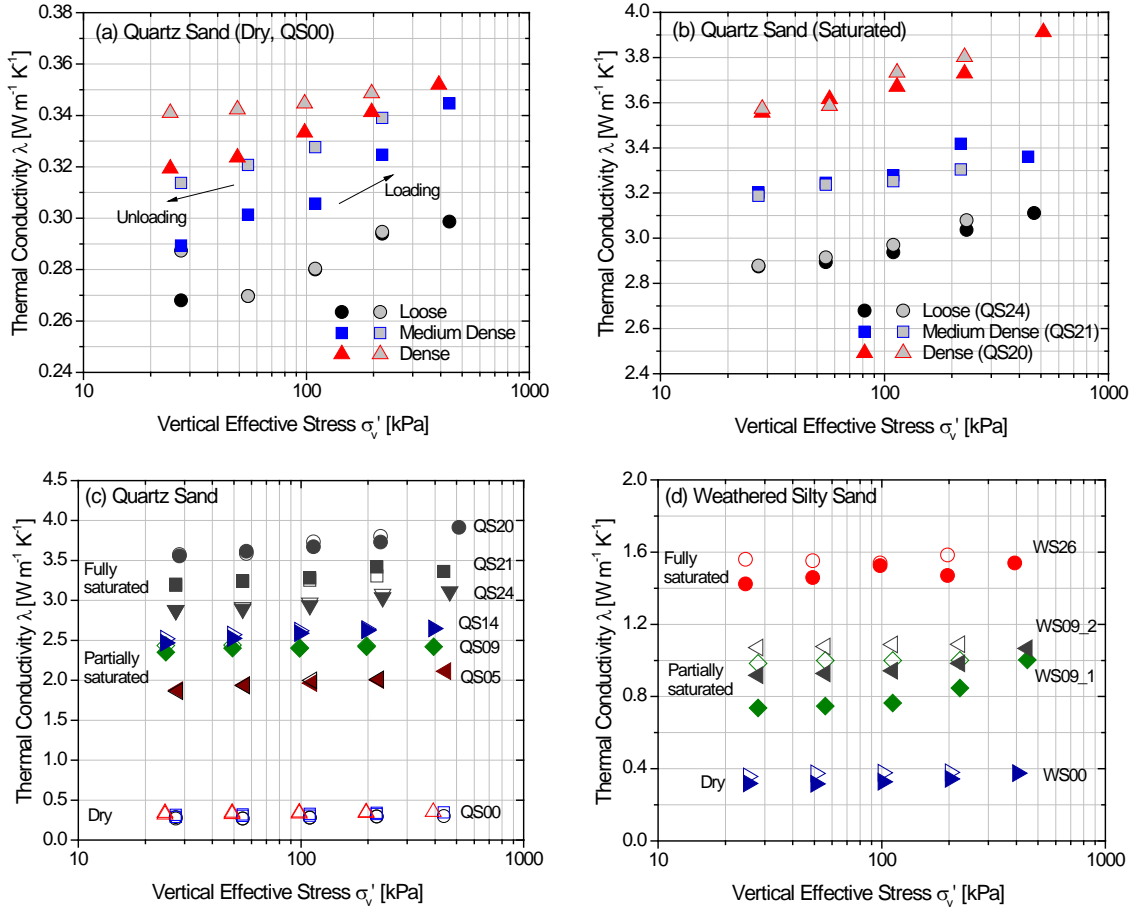
Fig. 3 The variances in thermal conductivity with respect to vertical effective stress: (a) dry quartz sand specimens; (b) saturated quartz sand specimens; (c) all quartz sand specimens; and (d) all weathered silty sand specimens

3.2 Variations in thermal conductivity λ with porosity ϕ

Figs. 4(a) and (b) show the results of the dry and saturated quartz sand specimens with three different initial compacted states: loose, medium dense, and dense specimens. Initial dry thermal conductivity λ_{dry} before loading was observed to increase with the initial density, which corroborates the work by Yun and Santamarina (2008). The same trend was confirmed for the saturated specimens; the highest λ_{sat} was observed for the dense specimen, and the lowest λ_{sat} for the loose specimen. The dry thermal conductivity increased from $\lambda_{dry} = 0.26$ W·m^{-1}·K^{-1} for $\phi = 0.41$ to $\lambda_{dry} = 0.35$ Wm^{-1}·K^{-1} for $\phi = 0.34$ (refer to Table 3). The saturated thermal conductivity increased from $\lambda_{sat} = 2.85$ W·m^{-1}·K^{-1} for $\phi = 0.39$ to $\lambda_{sat} = 3.91$ W·m^{-1}·K^{-1} for $\phi = 0.31$ (refer to Table 3). The dry thermal conductivity λ_{dry} and the saturated thermal conductivity λ_{sat} were found to decrease linearly with increasing porosity ϕ, as can be seen in Figs. 4(a) and (b).

Figs. 4(c) and (d) show the variations in thermal conductivity λ with porosity ϕ for all specimens of the quartz sand and weathered silty sand, respectively. For all cases, it was confirmed
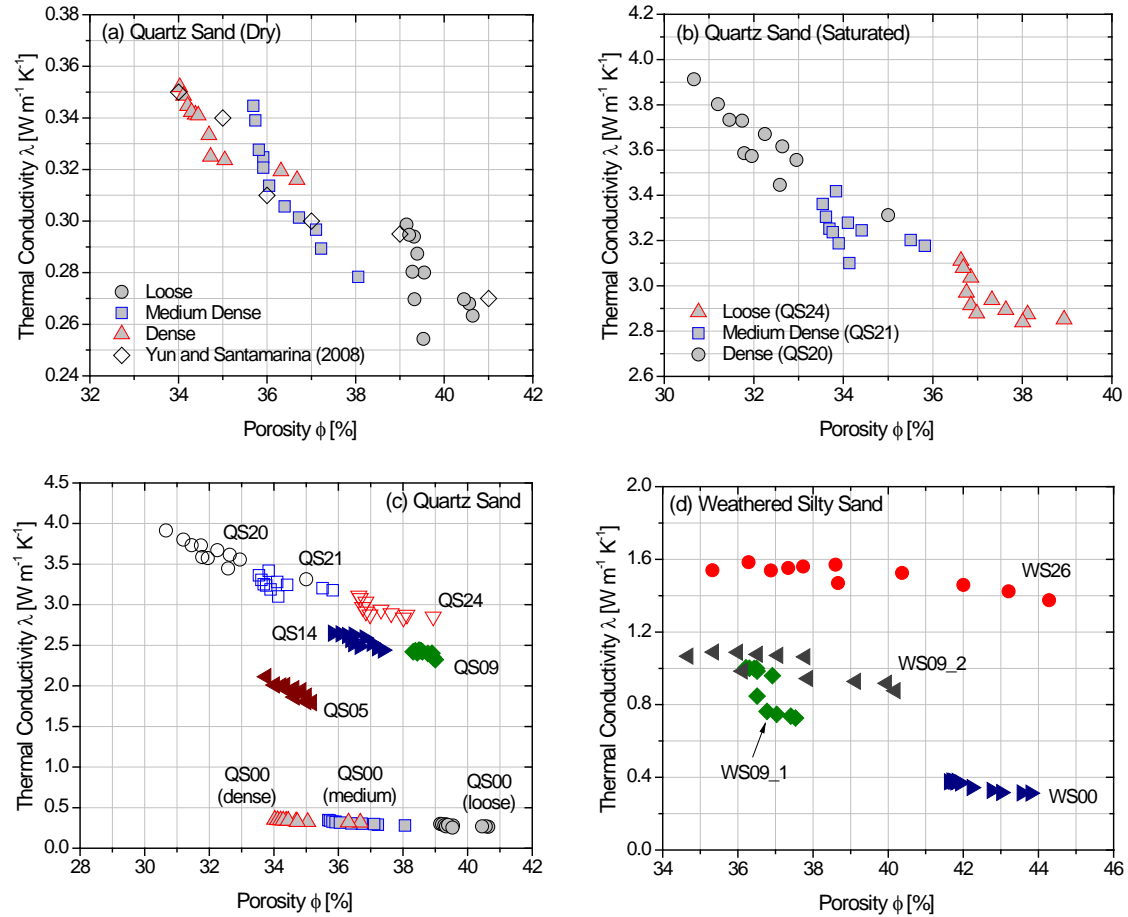
Fig. 4 The variances in thermal conductivity with respect to porosity: (a) dry quartz sand specimens; (b) saturated quartz sand specimens; (c) all quartz sand specimens; and (d) all weathered silty sand specimens

that the thermal conductivity λ generally increased as the porosity ϕ decreased though the variations depended on water content (or water saturation), soil type, and effective stress. It particularly appears that the extent of thermal conductivity increase with decreasing porosity was less distinct in the weathered silty sand (Fig. 4(d) or Table 4), compared to that in quartz sand (Fig. 4(c) or Table 3). It is presumably attributed to the fact that the weathered silty sand had the lower thermal conductivity of solid minerals than the quartz sand did.

3.3 Effect of water saturation S on thermal conductivity λ

Fig. 5 shows the measured thermal conductivity λ plotted against water saturation S. Herein, the water saturation S was defined as the water volume divided by the pore volume and was calculated from the porosity ϕ, water content w, and specific gravity G_s (i.e., $S = G_s \cdot w \cdot (1 - \phi) / \phi$). For the quartz sand sample, the thermal conductivity λ increased from ~0.26–0.35 W·m^{-1}·K^{-1} to ~2.84–3.91 W·m^{-1}·K^{-1} as the water saturation S increased from 0% to 100% (refer Fig. 5(a)). For the
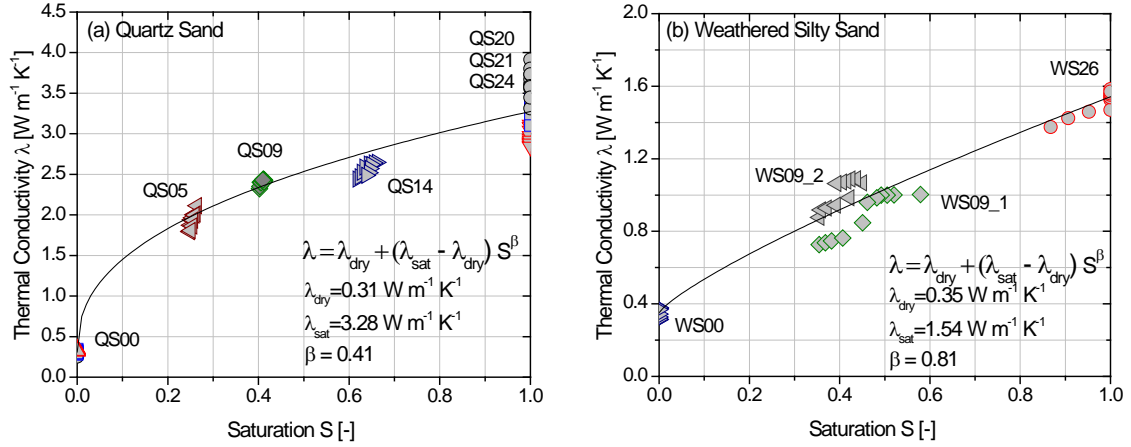
Fig. 5 The obtained relations of the thermal conductivity versus (a) water saturation for quartz sand; and (b) weathered silty sand

weathered silty sand sample, the thermal conductivity λ increased from ~0.31–0.38 W·m^{-1}·K^{-1} to ~1.38–1.58 W·m^{-1}·K^{-1} as the water saturation S increased from 0% to 100% (refer Fig. 5(b)). It is clear that the water saturation S had a much higher effect of the thermal conductivity λ than the other properties (e.g., effective stress and porosity), increasing λ by almost one order of magnitude. It was observed that the λ-S relation was non-linear in the quartz sand; however, it was fairly linear in the weather silty sand. While the dry thermal conductivities λ_{dry} of the quartz sand and weathered silty sand ranged the similar with the difference less than 0.1 mW^{-1}·K^{-1}, it was particularly noted that the saturated thermal conductivities λ_{sat} of the quartz sand (e.g., 2.85–3.91 W·m^{-1}·K^{-1}) was considerably greater than that of the weathered silty sand (e.g., 1.38–1.58 W·m^{-1}·K^{-1}). It is possibly because the thermal conductivity of solid minerals of the weathered silty sand (e.g., λ_s = ~4.71 W·m^{-1}·K^{-1}) was much lower than that of the quartz sand (e.g., λ_s = ~7.69 W·m^{-1}·K^{-1}); the weathered silty sand was composed of several different minerals, including albite and biotite that were known to have low thermal conductivity (See Table 2).

4. Discussion

4.1 An improved model for predicting thermal conductivity

Among the factors that affect thermal conductivity λ, including the mineral composition, effective stress σ', porosity ϕ, and water saturation S, it was found that the water saturation S caused the highest variance in thermal conductivity λ. Furthermore, while the range of porosity ϕ in field conditions is fairly narrow (e.g., ϕ = 0.3–0.5 for soils), the *in situ* water saturation S can vary in the extreme cases from 0 to 1. Therefore, an improved empirical model for thermal conductivity prediction is suggested as follows

$$\lambda = \lambda_{dry} + (\lambda_{sat} - \lambda_{dry}) \cdot S^{\beta}, \tag{1}$$

where λ_{dry} and λ_{sat} are the thermal conductivity of the dry soil and saturated soil, respectively. S is the water saturation and β is the fitting parameter that represents the curvature of the λ-S graph. A

value of fitting parameter $\beta = 1$ indicates a linear λ-S relation; the λ-S relation will be a convex curve when $\beta < 1$, and a concave curve when $\beta > 1$. Fig. 5 shows the suggested model results fitted for the compiled λ-S data of the soil samples. For the quartz sand sample, the following parameters were used: $\lambda_{dry} = 0.31$ W·m^{-1}·K^{-1}, $\lambda_{sat} = 3.28$ W·m^{-1}·K^{-1} and $\beta = 0.41$. For the weathered silty sand sample, the following parameters were used: $\lambda_{dry} = 0.35$ W·m^{-1}·K^{-1}, $\lambda_{sat} = 1.54$ W·m^{-1}·K^{-1}, and $\beta = 0.81$. Accordingly, the lower value of β for the quartz sand sample showed that the λ-S curve is more concave, whereas, for the silty sand sample, the β parameter was close to 1, which resulted in a fairly linear λ-S curve, as can be seen in Fig. 5. Aforementioned, as the effective stress in the moderate range of several hundreds kPa was proven to change the thermal conductivity by ~25% at the most (Fig. 3 and Tables 3 and 4), it is worth noting that the suggested model does not consider the effective stress; thus, caution is advised when the suggested model is used.

　　Semi-theoretical models (e.g., series and parallel models for the three components; Hashin-Shtrikman upper and lower bounds; Hashin and Shtrikman 1963) and empirical models suggested by previous researchers (e.g., Kersten 1949, Johansen 1977, Côté and Konrad 2005, Lu *et al.* 2007) were superimposed in Fig. 6 for comparison. Table 5 presents the semi-theoretical and empirical models used in this study. Table 6 summarizes the input parameters used for the prediction models. It was observed that the parallel model acted as the upper bound and the series model acted as the lower bound in addition to the Hashin–Shtrikman (HS) upper and lower bounds. These bounds were placed far above or below the experimental data for the both samples. The empirical models including those by Kersten (1949), Johansen (1977), Côté and Konrad (2005), and Lu *et al.* (2007) also showed poor agreement with the experimental results. The model by Côté and Konrad (2005) predicted a concave λ-S relation, which was not entirely suitable for our results. The models by Johansen (1977) and Lu *et al.* (2007) produced similar λ-S relations in the mid-range of water saturation S (e.g., 30–70%); however, the dry and saturated thermal conductivities (λ_{dry} and λ_{sat}) were poorly predicted. Therefore, it was confirmed that deriving one generalized semi-theoretical model applicable to all types of soils appears to be nearly impracticable, mainly because of the difficulty in predicting dry and saturated thermal conductivities (λ_{dry} and λ_{sat}). Hence, it was concluded that the suggested model using experimentally determined dry and saturated thermal conductivities (λ_{dry} and λ_{sat}) would be more versatile.
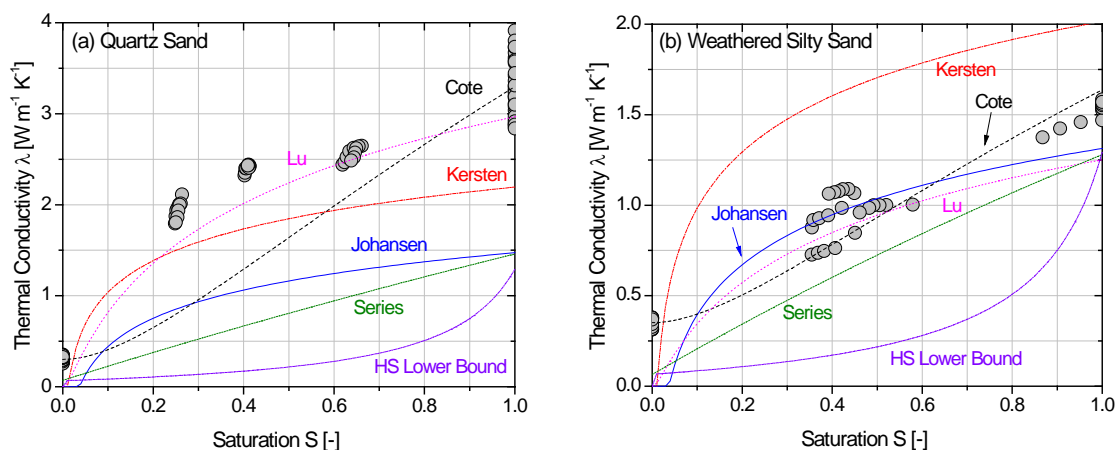

Fig. 6 Comparisons of the test results with semi-theoretical and empirical models: (a) quartz sand; and (b) weathered silty sand

Table 5 Thermal conductivity estimation models

Model	Equation	Notation
Series	$$\lambda = \left[\left(\frac{\phi}{S/\lambda_{water} + (1-S)/\lambda_{air}} \right) + \left(\frac{1-\phi}{\lambda_s} \right) \right]^{-1}$$	Thermal conductivity of solid λ_s [W·m⁻¹·K⁻¹] Thermal conductivity of water λ_{water} [W·m⁻¹·K⁻¹] Thermal conductivity of air λ_{air} [W·m⁻¹·K⁻¹] Water saturation S [-] Porosity ϕ [-]
Parallel	$$\lambda = (S \cdot \lambda_{water} + (1-S)\lambda_{air}) \cdot \phi + \lambda_s \cdot (1-\phi)$$	
Hashin-Shtrikman upper bound	$$\lambda = \lambda_s \left(1 + \frac{3 \cdot (1-\phi) \cdot (\lambda_{VU} - \lambda_s)}{3\lambda_s + \phi \cdot (\lambda_{VU} - \lambda_s)} \right)$$	$$\lambda_{VU} = \lambda_{water} \left(1 + \frac{3 \cdot (1-S) \cdot (\lambda_{air} - \lambda_{water})}{3\lambda_{water} + S \cdot (\lambda_{air} - \lambda_{water})} \right)$$
Hashin-Shtrikman lower bound	$$\lambda = \lambda_{VL} \left(1 + \frac{3 \cdot \phi \cdot (\lambda_s - \lambda_{VL})}{3\lambda_{VL} + (1-\phi) \cdot (\lambda_s - \lambda_{VL})} \right)$$	$$\lambda_{VL} = \lambda_{air} \left(1 + \frac{3 \cdot S \cdot (\lambda_{water} - \lambda_{air})}{3\lambda_{air} + (1-S) \cdot (\lambda_{water} - \lambda_{air})} \right)$$
Kersten (1949)	$$\lambda = 0.1442(0.7\log_{10}(w\%) + 0.4) \cdot 10^{0.6243\rho_d}$$	Water content w [%] Dry density ρ_d [g/cm³]
Johansen (1977)	$$\lambda = (\lambda_{sat} - \lambda_{dry}) \cdot [0.7\log(S) + 1.0]$$ $$\lambda_{sat} = \lambda_s^{\phi} \cdot \lambda_{water}^{1-\phi}$$ $$\lambda_{dry} = (0.137\rho_d + 64.7)/(2700 - 0.974\rho_d)$$	Thermal conductivity of dry soil λ_{dry} [W·m⁻¹·K⁻¹] Thermal conductivity of saturated soil λ_{sat} [W·m⁻¹·K⁻¹] Dry density ρ_d [kg/m³]
Cote and Konrad (2005)	$$\lambda = (\lambda_{sat} - \lambda_{dry}) \cdot \left[\kappa S/(1 + (\kappa - 1)S) \right] + \lambda_{dry}$$ $$\lambda_{dry} = \chi \cdot 10^{-\eta\phi}$$	*The fitting parameters:* $\chi = 0.75$ W·m⁻¹·K⁻¹ $\eta = 1.2$ for natural mineral soil $\kappa = (4.7S)/(1+3.7S)$ for unfrozen coarse materials
Lu *et al.* (2007)	$$\lambda = (\lambda_{sat} - \lambda_{dry}) \cdot \exp\left[\alpha\left(1 - S^{(\alpha-1.33)}\right) \right]$$ $$\lambda_{dry} = -0.56 \cdot \phi + 0.51$$	*The fitting parameter:* $\alpha = 0.96$ Porosity ϕ [-]
This study	$$\lambda = \lambda_{dry} + (\lambda_{sat} - \lambda_{dry}) \cdot S^{\beta}$$	Water saturation S [-] *The fitting parameter:* β

Table 6 Input parameters for the thermal conductivity estimation models

Input parameter	Value
Thermal conductivity of water λ_{water} [W·m^{-1}·K^{-1}]	0.598 [a]
Thermal conductivity of air λ_{air} [W·m^{-1}·K^{-1}]	0.026 [b]
Thermal conductivity of solid λ_s [W·m^{-1}·K^{-1}]	7.69 for quartz sand [c] 4.71 for weathered silty sand [d]
Porosity ϕ [-]	0.36 for quartz sand [e] 0.39 for weathered silty sand [e]
Dry density ρ_d [g/cm^3]	1.696 for quartz sand [e] 1.617 for weathered silty sand [e]
Thermal conductivity of dry soil λ_{dry} [W·m^{-1}·K^{-1}]	0.31 for quartz sand [e] 0.35 for weathered silty sand [e]
Thermal conductivity of saturated soil λ_{sat} [W·m^{-1}·K^{-1}]	3.28 for quartz sand [e] 1.54 for weathered silty sand [e]

Note: [a] Cortes *et al.* (2009); [b] Andersland and Ladanyi (2004); [c] Horai and Simmons (1969);
[d] The value was obtained from the weighted average of those of the minerals from Table 2;
[e] The values were calculated by averaging the experiment results

5. Conclusions

This study explored the effects of geotechnical engineering properties on the thermal conductivity of soils. The thermal conductivity of quartz sands and weathered silty sands were documented via a series of laboratory experiments, and these were correlated with relevant engineering parameters to examine the effects of effective stress, porosity, and water saturation on thermal conductivity. The main findings are as follows:

- Thermal conductivity λ expectedly increased with an increase in effective stress σ' because of the increased grain-to-grain contact area and coordination number (or contact number), and the decreased porosity. The variation of λ caused by the effective stress increment of ~400–500 kPa was limited to ~10–25% for the particular tested soils (the quartz sand and weathered silty sand samples).
- The dry thermal conductivity λ_{dry} and the saturated thermal conductivity λ_{sat} were found to linearly decrease with increasing porosity ϕ. Moreover, at each water content, the thermal conductivity λ generally increased with decreasing porosity ϕ whereas the variations depended on the water content (or water saturation), soil type, and effective stress.
- It was experimentally confirmed that the water saturation S had a much more substantial effect on the thermal conductivity λ than the other properties (e.g., effective stress and porosity), increasing λ byalmost one order of magnitude. The λ-S relation was found to be significantly non-linear.
- For the particular class of the soils tested in this study, an improved model based on water saturation S, dry thermal conductivity λ_{dry}, saturated thermal conductivity λ_{sat}, and the fitting parameter β was suggested. This form of the prediction model using experimentally measured dry and saturated thermal conductivity (λ_{dry} and λ_{sat}) can be useful in spite of some limitations of not considering the effect of effective stress and porosity.

Acknowledgments

References

Andersland, O.B. and Ladanyi, B. (2004), *Frozen Ground Engineering*, (2nd Edition), John Wiley and Sons, Inc., 363 p.

ASTM D4253-14 (2014), *Standard Test Methods for Maximum Index Density and Unit Weight of Soils Using Vibratory Table*, ASTM International, West Conshohocken, PA, USA.

ASTM D4254-14 (2014), *Standard Test Methods for Minimum Index Density and Unit Weight of Soils and Calculation of Relative Density*, ASTM International, West Conshohocken, PA, USA.

ASTM D5334-14 (2014), *Standard Test Method for Determination of Thermal Conductivity by Thermal Needle Probe Procedure*, ASTM International, West Conshohocken, PA, USA.

Batchelor, G.K. and O'Brien, R.W. (1977), "Thermal or electrical conduction through a granular material", *Proceedings of the Royal Society of London. Series A*, *Mathematical and Physical Sciences*, **355**(1682), 313-333.

Brandl, H. (2006), "Energy foundations and other thermos-active ground structures", *Géotechnique*, **56**(2), 81-122.

Brigaud, F. and Vasseur, G. (1989), "Mineralogy, porosity and fluid control on thermal conductivity of sedimentary rocks", *Geophys. J. Int.*, **98**(3), 525-542.

Carslaw, H.S. and Jaeger, J.C. (1959), *Conduction of Heat in Solids*, (2nd Edition), Oxford University Press, London, 510 p.

Cortes, D.D., Martin, A.I., Yun, T.S., Francisca, F.M., Santamarina, J.C. and Ruppel, C. (2009), "Thermal conductivity of hydrate-bearing sediments", *J. Geophys. Res.*, **114**, B11103. DOI: 10.1029/2008JB006235

Côté, J. and Konrad, J. (2005), "A generalized thermal conductivity model for soils and costruction materials", *Can. Geotech. J.*, **42**, 443-458.

Esch, D.C. (2004), *Thermal Analysis*, *Construction and Monitoring Methods for Frozen Ground*, American Society of Civil Engineers, 492, Reston, VA, USA.

Gangadhara Rao, M.V.B.B. and Singh, D.N. (1999), "A generalized relationship to estimate thermal resistivity of soils", *Can. Geotech. J.*, **36**, 767-773.

Go, G.H., Lee, S.R., Kim, Y.S., Park, H.K. and Yoon, S. (2014), "A new thermal conductivity estimation model for weathered granite soils in Korea", *Geomech. Eng., Int. J.*, **6**(4), 359-376.

Gori, F. and Corasaniti, S. (2004), "Theoretical prediction of the thermal conductivity and temperature variation inside Mars soil analogues", *Planet. Space Sci.*, **52**, 91-99.

Hashin, Z. and Shtrikman, S. (1963), "A variational approach to the theory of the elastic behavior of multiphase materials", *J. Mech. Phys. Solids*, **11**(2), 127-140.

Horai, K.I. and Simmons, G. (1969), "Thermal conductivity of rock forming minerals", *Earth Planet. Sci. Lett.*, **6**(5), 359-368.

Johansen, O. (1977), *Thermal Conductivity of Soils*, Cold Regions Research and Engineering Lab Hanover NH, No. CRREL-TL-637.

Johnston, I.W., Narsilio, G.A. and Colls, S. (2011), "Emerging geothermal energy technologies", *KSCE J. Civ. Engrs.*, **15**(4), 643-653.

Kersten, M.S. (1949), "Laboratory research for the determination of the thermal properties of soils", ACFEL Tech. Rep. 23; University of Minnesota, Minneapolis, MI, USA.

Kumai, W., Hashimoto, I., Ohsawa, S., Mitani, M. and Matsuda, Y. (1994), "Completion of high-efficiency water pipe cooling system for underground transmission line", *IEEE Trans. Power Delivery*, **9**(1), 585-590.

Kumlutas, D., Tavman, I.H. and Coban, M.T. (2003), "Thermal conductivity of particle filled polyethylene composite materials", *Compos. Sci. Technol.*, **63**, 113-117.

Lu, S., Ren, T., Gong, Y. and Horton, R. (2007), "An improved model for predicting soil thermal conductivity from water content at room temperature", *Soil. Sci. Soc. Am. J.*, **71**(1), 8-14.

Manohar, K., Yarbrough, D.W. and Booth, J.R. (2000), "Measurement of apparent thermal conductivity by the thermal probe method", *J. Test. Eval.*, **28**(5), 345-351.

Murashov, V.V. and White, M.A. (2000), "Thermal conductivity of crystalline particulate materials", *J. Mater. Sci.*, **35**, 649-653.

Nasirian, A., Cortes, D.D. and Dai, S. (2015), "The physical nature of thermal conduction in dry granular media", *Geotech. Lett.*, **5**, 1-5.

Roshankhah, S. and Santamarina, J.C. (2014), "Engineered granular materials for heat conduction and load transfer in energy geotechnology", *Geotech. Lett.*, **4**(2), 145-150.

Singh, D.N. and Devid, K. (2000), "Generalized relationships for estimating soil thermal resistivity", *Experim. Therm. Fluid Sci.*, **22**, 133-143.

Sridhar, M.R. and Yovanovich, M.M. (1996), "Elastoplastic contact conductance model for isotropic conforming rough surfaces and comparison with experiments", *J. Heat Transfer*, **118**(1), 3-9.

Tarnawski, V.R., Leong, W.H., Gori, F., Buchan, G.D. and Sundberg, J. (2002), "Inter- particle contact heat transfer in soil systems at moderate temperatures", *Int. J. Energy Res.*, **26**, 1345-1358.

Van der Held, E.F.M. and Van Drunnen, F.G. (1949), "A method of measuring thermal conductivity of liquids", *Physica*, **15**(10), 865-881.

Vargas, W.L. and McCarthy, J.J. (2001), "Heat conduction in granular materials", *AIChE Journal*, **47**(5), 1052-1059.

Von Herzen, R. and Maxwell, A.E. (1959), "The measurement of thermal conductivity of deep-sea sediments by a needle-probe method", *J. Geophys. Res.*, **64**(10), 1557-1563.

Woodside, W.M.J.H. and Messmer, J.H. (1961), "Thermal conductivity of porous media. I. Unconsolidated sands", *J. Appl. Phys.*, **32**(9), 1688-1699.

Yun, T.S. and Santamarina, J.C. (2008), "Fundamental study of thermal conduction in dry soils", *Granul. Matter*, **10**(3), 197-207.

GC